

# Classical Approximation for Ionization by Proton Impact\*

J. D. GARCIA† AND E. GERJUOY

*Department of Physics, University of Pittsburgh, Pittsburgh, Pennsylvania*

AND

JEAN E. WELKER

*National Aeronautical Space Administration—Goddard Space Flight Center, Greenbelt, Maryland*

(Received 14 July 1967)

Ionization of atoms by proton impact, as predicted by the classical binary-encounter approximation, is examined and compared with available experimental data on the noble-gas and alkali-metal atoms. The results indicate that these predictions agree with observation to within a factor of 2 or 3, and are as reliable as the comparable results for electron ionization. Comparisons are made between electron and proton ionization cross sections. The proton ionization curves all have a single maximum and are otherwise monotonic, in contrast to electron ionization, where the effects of atomic shell structure produce secondary maxima for some atoms. The effect of averaging over bound-state speed distributions is discussed, and is found to be much less important for protons than for electrons, except at very low proton energies. The need for experimental measurements at higher energies ( $\sim 10$  MeV) is discussed.

## I. INTRODUCTION

THE classical binary-encounter approximation has been quite successful in predicting inelastic-electron-collision cross sections for atomic and molecular systems.<sup>1,2</sup> In this study, we examine the utility of this method as applied to ionization by heavy-particle impact, in particular, by proton impact. We have avoided approximations, other than those dictated by the model, in an attempt to obtain a clear assessment of its applicability to the processes considered. The principal advantage of the method is the ease of calculation of the cross sections. However, the classical approximation is not completely lacking in theoretical justification, since—for ionization, at any rate—it has been shown<sup>3</sup> to be intimately related to a quantum theoretical treatment.

Section II describes the formulation, and Sec. III presents the results and discussion. It is found that in the noble gases the classical description of ionization by proton impact is as reliable as that for electron impact (i.e., to within a factor of 2 or 3). Though we have not studied such cases, it is probable, as Gryzinski's original papers suggest, that the agreement for proton ionization in diatomic molecules is about as good.

## II. CLASSICAL IONIZATION CROSS SECTIONS

The binary-encounter model is based on the assumption that the determining interaction is that between the incident particle and the bound atomic electrons. It requires a knowledge of the differential cross section,

$\sigma_{\Delta E}^{\text{eff}}(v_1, v_2; m_1/m_2)$ , for the exchange of energy  $\Delta E$  in the laboratory frame between an incident particle of mass  $m_1$  and velocity  $v_1$ , and the bound electron whose velocity is  $v_2$ , averaged over all orientations of  $v_2$ . The ionization cross section for protons incident upon an atom would then be given by

$$\sigma_{\text{ion}} = \sum_i n_i \int_{u_i}^{E_1} \sigma_{\Delta E}^{\text{eff}}\left(v_1, v_2; \frac{m_p}{m_e}\right) d\Delta E, \quad (1)$$

where  $n_i$  is the number of electrons having ionization energy  $u_i$ , and  $E_1$  is the incident proton energy. The resultant cross section is then to be averaged over the speed distributions of the bound electrons,  $f(v_2)dv_2$ .

This model was first proposed by Gryzinski.<sup>1</sup> It has proved to be quite reliable in predicting electron-collision cross sections, agreeing with experiment to within a factor of about 2 or 3, often much better.<sup>2</sup> However, Gryzinski's formulation of the problem contains a number of simplifying assumptions; furthermore, his final expressions for the cross sections have been averaged over velocity distributions for the atomic electrons which at best have merely semiempirical merit. It may be that Gryzinski's simplifying assumptions often produce slightly better agreement with experiment. Nevertheless, in this paper we prefer to examine the predictions of the classical binary-encounter model for proton ionization without additional assumptions. It appears, however, that Gryzinski's simplifying assumptions do not change the predictions by a factor greater than 1.5.

In the case of electron impact ionization, the exact expression corresponding to (1) was given by Gryzinski and has been rederived by Stabler,<sup>4</sup> and the effect of averaging over the correct atomic velocity distribution for hydrogen was examined by Kingston.<sup>5</sup> The expression for  $\sigma_{\Delta E}^{\text{eff}}$  for unequal mass particles given by

\* Research supported in part by the Advanced Research Projects Agency under Contract No. DA-31-124-ARO-D-440 and in part by the National Aeronautics and Space Administration under Contract No. NGR-39-011-035.

† Present address: Department of Physics, University of Arizona, Tucson, Ariz.

<sup>1</sup> M. Gryzinski, Phys. Rev. **115**, 374 (1959); **138**, A305 (1965); **138**, A322 (1965); **138**, A336 (1965).

<sup>2</sup> E. Bauer and C. D. Bartkey, J. Chem. Phys. **43**, 2466 (1965).

<sup>3</sup> J. D. Garcia, Phys. Rev. **159**, 39 (1967).

<sup>4</sup> R. C. Stabler, Phys. Rev. **133**, A1286 (1964).

<sup>5</sup> A. E. Kingston, Phys. Rev. **135**, A1637 (1964).

Gryzinski contains some approximations. Gerjuoy<sup>6</sup> has derived the exact expression for this case, and his

closed-form expressions are readily integrable. The final results are, for  $m_1 > m_2$  and  $\Delta E > 0$ ,

$$\begin{aligned} \int^{\Delta E} \sigma_{\Delta E}^{\text{eff}}\left(v_1, v_2; \frac{m_1}{m_2}\right) d\Delta E &= \frac{1}{3}\pi \frac{(z_1 z_2 e^2)^2}{v_1^2 v_2} \left[ -\frac{2v_2^3}{(\Delta E)^2} - \frac{6v_2/m_2}{\Delta E} \right], \quad 0 < \Delta E < b \\ &= \frac{1}{3}\pi \frac{(z_1 z_2 e^2)^2}{v_1^2 v_2} \left\{ \left(\frac{2}{m_1}\right)^2 \frac{v_1 - 2v_1'}{(v_1 - v_1')^2} + \left(\frac{2}{m_2}\right)^2 \frac{v_2 + 2v_2'}{(v_2 + v_2')^2} \right\}, \quad b < \Delta E < a \\ &= \frac{1}{3}\pi \frac{(z_1 z_2 e^2)^2}{v_1^2 v_2} \left[ -\frac{2v_1'^3}{(\Delta E)^2} \right], \quad (\Delta E > a \text{ and } 2m_2 v_2 > |m_1 - m_2| v_1) \\ &= 0, \quad (\Delta E > a \text{ and } 2m_2 v_2 < |m_1 - m_2| v_1) \end{aligned} \quad (2)$$

where

$$v_1' = (v_1^2 - 2\Delta E/m_1)^{1/2}, \quad v_2' = (v_2^2 + 2\Delta E/m_2)^{1/2},$$

$$a = [4m_1 m_2 / (m_1 + m_2)^2] [E_1 - E_2 + \frac{1}{2} v_1 v_2 (m_1 - m_2)],$$

and

$$b = [4m_1 m_2 / (m_1 + m_2)^2] [E_1 - E_2 - \frac{1}{2} v_1 v_2 (m_1 - m_2)].$$

These expressions, when used in (1), give the exact classical binary-encounter ionization cross section for protons of energy  $E_1$  impinging upon atoms whose electrons have speeds  $v_2$ , and are in spherically symmetrical states. They should be averaged over the speed distributions of the atomic electrons. For subshells whose electron distributions are not spherically symmetrical, a new  $\sigma_{\Delta E}^{\text{eff}}$  corresponding to the particular angular distribution involved would have to be derived (e.g., via the methods of Ref. 6).

The averaging over hydrogenic speed distributions can be done analytically, in terms of an infinite, convergent power series (see Ref. 3 for the leading terms in this series in the case of electron ionization in hydrogen). However, the expressions are quite simple to program for numerical evaluations of the integrals. By setting  $v_{2i} = (2u_i/m_e)^{1/2}$ , we obtain the expressions for a  $\delta$ -function speed distribution  $f(v_{2i}) \sim \delta[v_{2i} - (2u_i/m_e)^{1/2}]$ . In either case, the results will scale; that is, given one set of values for  $\sigma_{\text{ion}}(E_1, u_a)$  for a single electron whose binding energy is  $u_a$ , we can find those for an electron of ionization potential  $u_b$  as follows:

$$\sigma_{\text{ion}}(E_1', u_b) = (u_a^2/u_b^2) \sigma_{\text{ion}}(E_1, u_a), \quad (3)$$

where

$$E_1' = (u_b/u_a) E_1.$$

In the Appendix we give the complete expression for the ionization cross section corresponding to the  $\delta$ -function distribution. Needless to say, the ionization cross section for any given atom will, in general, bear no simple relation to those of any other atoms because of the different energies of the electronic shells, remembering

that all shells contribute to the total ionization cross section.

### III. RESULTS AND DISCUSSION

A large number of ionization reactions have been examined. We present only a representative sample. All results show the same qualitative features: the cross section rises gradually to a maximum, falls off as  $1/E$  thereafter. The onset of  $1/E$  behavior is much sooner after the maximum than is the case for electrons.

The first ionization potentials used are from Ref. 7; Ref. 8 was used for inner shell energies.

#### A. Hydrogen Atom

Figure 1 depicts the cross section for ionization of hydrogen atoms in the ground state by proton impact.

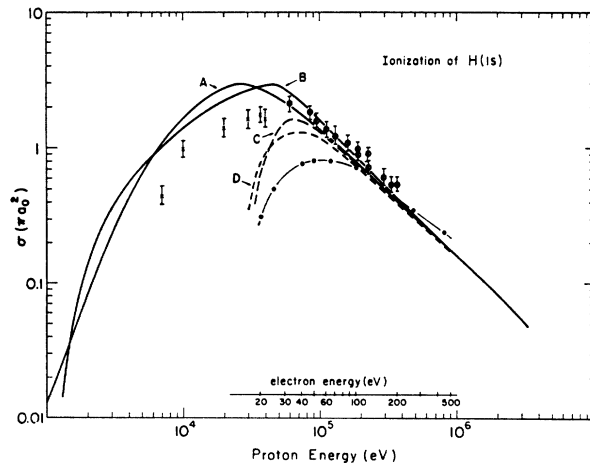


FIG. 1. Ionization of hydrogen. Curve A, classical proton cross section using correct velocity distribution; curve B, classical proton cross section using  $\delta$ -function distribution; curve C, classical electron cross section with  $\delta$ -function distribution; curve D, classical electron cross section, correct velocity distribution; crosses, experimental proton data (Ref. 9); crossed circles, experimental proton data (Ref. 10); full circles, experimental electron data (Ref. 11).

<sup>6</sup> E. Gerjuoy, Phys. Rev. **148**, 54 (1966).

<sup>7</sup> Natl. Bur. Std. (U. S.) Circ. No. 467 (1948), Vols. I and II.

<sup>8</sup> J. A. Beardon, Rev. Mod. Phys. **39**, 125 (1967).

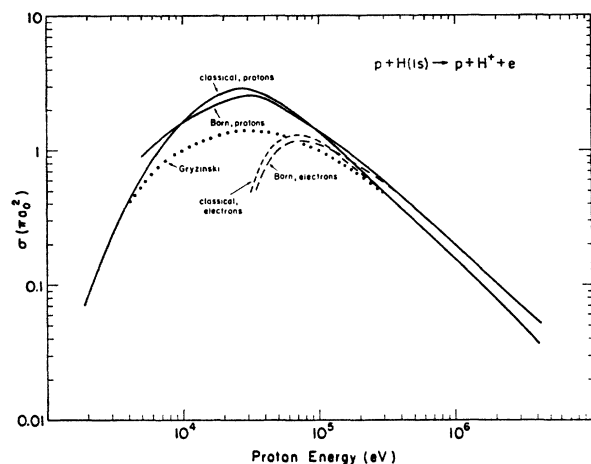


FIG. 2. Comparison of classical and Born approximations for ionization of hydrogen by protons (solid curves) and electrons (dashed curves) at equal velocities. The Born results are from Refs. 12 and 13. The dotted curve is the Gryzinski prediction (Ref. 1).

The data are from Refs. 9 and 10. Since in this case the exact velocity distribution is known, both  $\delta$ -function and exact-velocity distributions have been used. The corresponding results for impact of electrons at the same velocity are also shown for comparison.<sup>5,11</sup> It is evident that averaging over the correct velocity distribution has even less effect for protons. Since protons are in some sense more classical than electrons, it is perhaps no surprise that the predictions for proton ionization agree better with experiment.

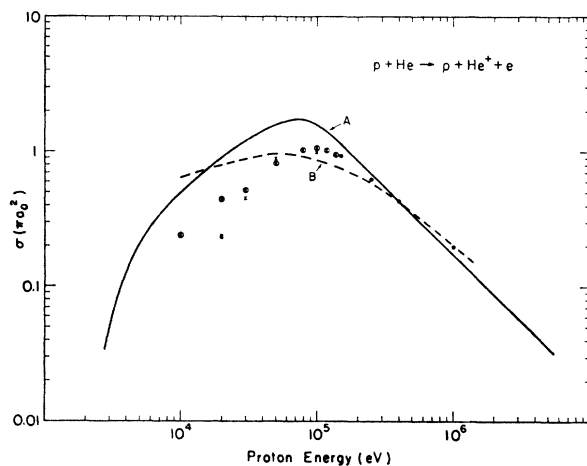


FIG. 3. Ionization of helium by proton impact. Curve A, present results; curve B, Born approximation (Ref. 14); crosses, experiment, Fedorenko *et al.* (Ref. 15); full circles, experiment McDaniel *et al.* (Ref. 15); crossed circles, experiment, De Heer *et al.* (Ref. 16).

<sup>9</sup> W. L. Fite, R. F. Stebbings, D. G. Hummer, and R. T. Brackmann, *Phys. Rev.* **119**, 663 (1960).

<sup>10</sup> J. V. Ireland and H. B. Gilbody, *Proc. Roy. Soc. (London)* **A277**, 137 (1964).

<sup>11</sup> W. L. Fite and R. T. Brackmann, *Phys. Rev.* **112**, 1141 (1958).

Figure 2 shows the comparison with the Born approximation<sup>12,13</sup>; in this figure, for both protons and electrons, the classical predictions have been averaged over the correct distribution. We have also included Gryzinski's original proton-ionization cross section.<sup>1</sup> The values from Ref. 1 shown in Fig. 2 are those averaged over Gryzinski's exponential speed distribution. Though it is not clear from Fig. 2, the Gryzinski curve has  $(\ln E)/E$  behavior at high energies.<sup>1</sup> Comparison of the present results using the  $\delta$ -function speed distribution with Gryzinski's corresponding values (not shown) shows that his values are 45% low at maximum, and about 30% high at 600 keV. These deviations are presumably the result of the approximations Gryzinski uses for the energy-exchange cross section.

Because the classical cross section is scalable, no new predictions would result for ionization of excited states of hydrogen. In accord with the results of Ref. 3, we

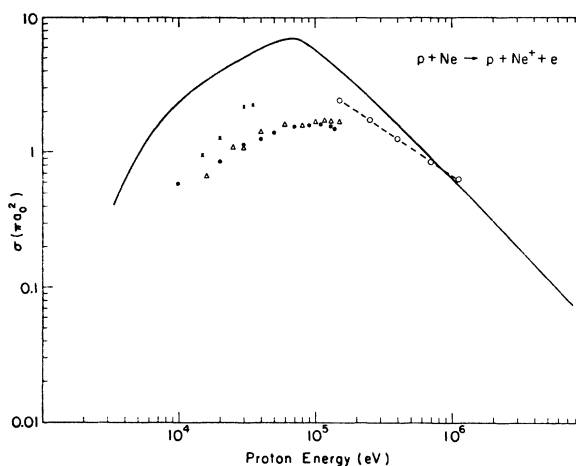


FIG. 4. Ionization of neon by proton impact. Solid curve, present results; open circles, McDaniel *et al.* (Ref. 15); triangles, Fedorenko *et al.* (Ref. 15); crosses, Hasted and Gilbody (Ref. 15); full circles, De Heer *et al.* (Ref. 16).

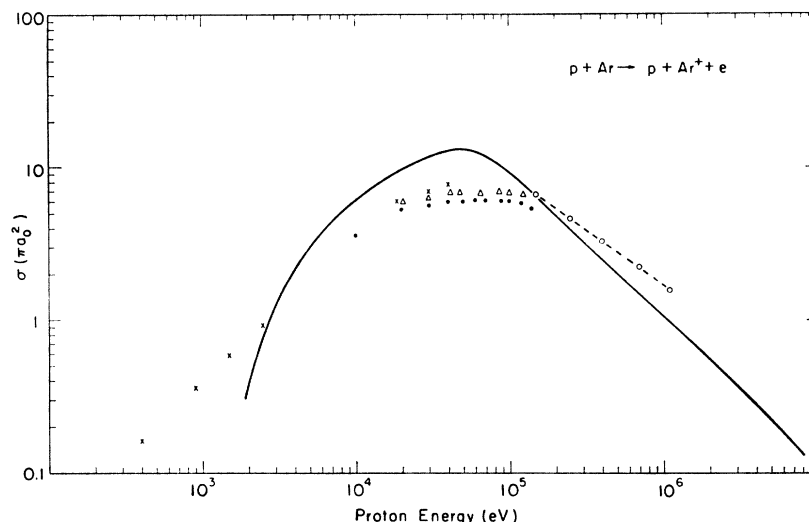
expect the Born-approximation results to approach our results as the principal quantum number increases; however, no Born calculations for excited state ionization by protons are known to us. It should be noted that for sufficiently large velocities, electrons and protons have equal ionization cross sections at equal velocities, whether in the Born or classical approximation (see the Appendix). Thus, for large energies, the arguments of Ref. 3 apply equally well to the ionization of hydrogen by proton impact.

At proton energies less than  $E_1 \sim 78u$ , the  $\delta$ -function distribution would predict a zero cross section (see the Appendix). This is a consequence of the fact that a slow heavy particle cannot classically transfer a large fraction of its energy to a lighter one. Averaging over the cor-

<sup>12</sup> D. R. Bates and G. Griffing, *Proc. Phys. Soc. (London)* **A66**, 961 (1953).

<sup>13</sup> K. Omidvar, *Phys. Rev.* **140**, A26 (1965).

FIG. 5. Ionization of argon by proton impact. Solid curve, present results; crosses, Gilbody and Hasted (Ref. 15); triangles, Fedorenko *et al.* (Ref. 15); open circles, McDaniel *et al.* (Ref. 15); full circles, De Heer *et al.* (Ref. 16).



rect velocity distribution corrects this false cutoff, though the cross section is quite small in the region  $u < E_1 < 78u$ .

Because the result of averaging over a hydrogenic distribution is so similar to the  $\delta$ -function results, we have used only  $\delta$ -function distributions in the remainder of our comparisons.

### B. Noble Gases

Figures 3–6 show the noble-gas proton ionization cross sections. For helium (Fig. 3), we also show the Born-approximation results.<sup>14</sup> The data were taken from Refs. 15–17. It can be seen that the factor of 2 or 3

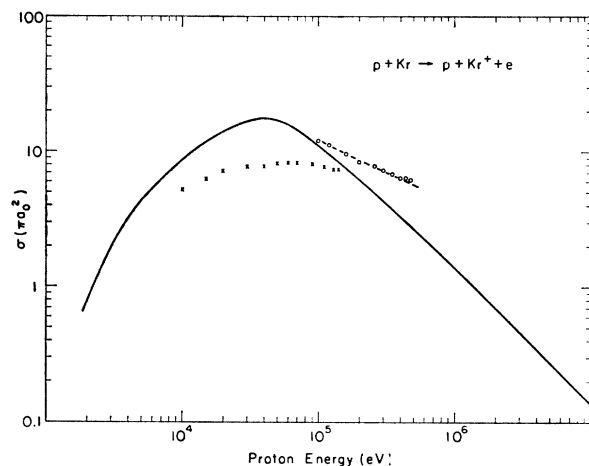


FIG. 6. Ionization of krypton by proton impact. Solid curve, present results; circles, Gilbody and Lee (Ref. 17); crosses, De Heer *et al.* (Ref. 16).

<sup>14</sup> R. A. Mapleton, Phys. Rev. **109**, 1166 (1958).

<sup>15</sup> Earl W. McDaniel, *Collision Phenomena in Ionized Gases* (John Wiley & Sons, Inc., New York, 1964), Chap. 6.

<sup>16</sup> F. J. De Heer, J. Schutten, and H. Moustafa, Physica **32**, 1766 (1966).

<sup>17</sup> H. B. Gilbody and A. R. Lee, Proc. Roy. Soc. (London) **A274**, 365 (1963).

agreement found for electron impact is approximately true here also. We see that at higher energies the data and the theoretical curves differ in slope, as indicated by the dashed lines in Figs. 4–6, implying possible larger disagreement for much higher energies; we discuss this matter further in Sec. IV.

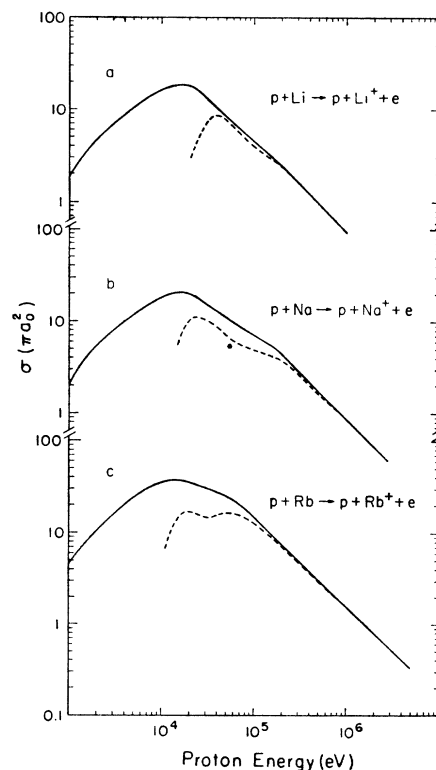


FIG. 7. Ionization of alkali atoms. Solid curves are the proton ionization cross sections; dashes denote cross section for electrons with equal velocity: (a) lithium atoms; (b) sodium atoms; (c) rubidium atoms.

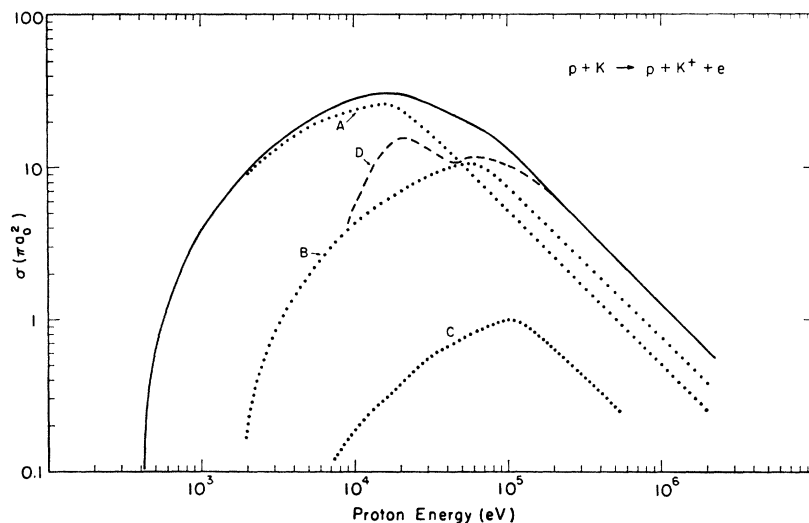


FIG. 8. Ionization of potassium. Solid curve, total proton ionization cross section; curve A, contribution from 4s subshell; curve B, contribution from 3p subshell; curve C, contribution from 3s subshell; curve D (dashes), total electron ionization cross section at equal impact velocities.

### C. Alkali Atoms

The alkali sequence provides an interesting example of the dissimilarity between electron and proton ionization cross sections. For electron ionizations in the heavier alkali-metal atoms, the inner-shell contributions soon dominate and produce secondary maxima.<sup>18</sup> The differences between the electron and proton cases are due to the different rates at which the curves increase with increasing energy above threshold. Figures 7 and 8 show that the proton curves are all smooth functions with single maxima. We have given the classical electron cross sections for comparison; these classical electron cross sections predict well all qualitative features and are within a factor of about 2 of the experimental results.<sup>18</sup> For potassium, we show the inner-shell contributions separately. We know of no proton-ionization data with which to compare our results.

### IV. SUMMARY

In all cases examined, ionization by proton impact proved to be about as reliably predicted by the classical binary-encounter theory as were the corresponding electron-impact results.<sup>2</sup>

Despite this numerical agreement in the range of impact energies presently available, we find some evidence indicating that at higher energies, larger discrepancies may occur. The trend in the experimental values for the noble-gas sequence appears to indicate that the classical approximation is less reliable at higher energies as the number of electrons in the system increases. It can be observed that the slope of the experimental values (dashed lines) in Figs. 3-6 increases as  $Z$  gets larger, and at krypton is consistent with a  $1/\sqrt{E}$  decrease at the higher measured energies. This is somewhat at variance with the high-energy Born  $(\ln E)/E$  prediction; there is, of course, good agreement between

the Born approximation and binary-encounter values (see Figs. 2 and 3) for small systems. A detailed comparison of the present model and Born approximation for a large system is warranted, but has not yet been carried out. In any case, it is our conclusion that measurements of these cross sections at higher energies ( $E \sim 10$  MeV) will be necessary to establish their true high-energy behavior. It should be mentioned that the experimental values herein quoted for the noble gases are, in fact, electron production cross sections rather than ionization cross sections. This is important at higher energies because some inner-shell contributions, though never dominant for the noble gases, do come well within a factor of 10 of the outermost  $p$ -shell contributions. These inner-shell ionizations are invariably followed by several Auger transitions, enhancing the electron production cross section. The enhancement due to subsequent Auger processes can be experimentally found by a determination of the energy distribution of the ejected electrons; such processes lead to sharply peaked distributions, unlike the ionization distribution which is much broader. A proper comparison of theoretical and experimental ionization cross sections would include subtraction of the Auger enhancement from the electron production cross sections.

### APPENDIX

Here we state the result of using the integrals (2) in the expression for the cross section for ionization of one electron whose binding energy is  $u$  by a charged particle of mass  $m_1 > m_e$ . We give only the result for  $\frac{1}{2}m_e v_2^2 = u$ , corresponding to a  $\delta$ -function velocity distribution, because it is deemed the most useful. The form for  $\frac{1}{2}m_e v_2^2 \neq u$  is as easily obtained from (2), if desired.

In order to facilitate its application, we present the result in terms of the velocity ratio,  $\alpha = v_1/v_2$ . Let  $q_0 = (z_1 z_2 e^2)^2$ ,  $\lambda = m_e/m_1$ ; in this notation,  $E_1 = (\alpha^2/\lambda)u$ .

<sup>18</sup> J. D. Garcia, J. Chem. Phys. (to be published).

For protons on electrons,  $z_1 = z_2 = 1$ . The cross section is:

(a) for  $1 > \lambda \geq (3 - 2\sqrt{2})$ :

$$\begin{aligned} \sigma_{\text{ion}} &= 0, & \text{for } \alpha < \sqrt{\lambda} \\ &= \frac{2\pi q_0}{3 u^2} \frac{(\alpha^2 - \lambda)^{3/2}}{\alpha^2}, & \text{for } \sqrt{\lambda} < \alpha < \frac{\lambda - 1 + \sqrt{2}(1 + \lambda)}{2} \\ &= \frac{\pi q_0}{3 u^2} \frac{1}{\alpha^2} \left\{ \frac{\lambda^2(1 + \lambda)}{2} \left[ \frac{3\alpha(1 + \lambda) - 4\lambda(\alpha + 1)}{4(\alpha - \lambda)^2} \right] + (1 + \lambda) \frac{4(\alpha + 1) - (\lambda + 1)}{8(\alpha + 1)^2} - \frac{\lambda^2}{2} \frac{\alpha - 2(\alpha^2 - \lambda)^{1/2}}{[\alpha - (\alpha^2 - \lambda)^{1/2}]^2} - \frac{1 + 2\sqrt{2}}{2(3 + 2\sqrt{2})} \right. \\ &\quad \left. + \frac{(1 + \lambda)[\alpha(\lambda - 1) + 2\lambda]^3}{8(\alpha + 1)^2(\alpha - \lambda)^2} \right\}, & \text{for } \frac{\lambda - 1 + \sqrt{2}(1 + \lambda)}{2} < \alpha < \frac{2\lambda}{1 - \lambda} \\ &= \frac{\pi q_0}{3 u^2} \frac{1}{\alpha^2} \left[ \frac{3}{8} \frac{(1 + \lambda)^2}{\alpha + 1} - \frac{1 + 2\sqrt{2}}{2(3 + 2\sqrt{2})} - \frac{\lambda^2}{2} \frac{\alpha - 2(\alpha^2 - \lambda)^{1/2}}{[\alpha - (\alpha^2 - \lambda)^{1/2}]^2} \right], & \text{for } \frac{2\lambda}{1 - \lambda} < \alpha < \frac{1 - \lambda + \sqrt{2}(1 + \lambda)}{2} \\ &= \frac{\pi q_0}{3 u^2} \frac{1}{\alpha^2} \left[ 5 + \frac{3}{8} \frac{(1 + \lambda)^2}{\alpha + 1} + \frac{1 + \lambda}{2} \left( \frac{\alpha - \lambda(3\alpha - 4)}{4(\alpha - 1)^2} - \frac{4\alpha - 1 + 3\lambda}{4(\alpha + \lambda)^2} \right) \right. \\ &\quad \left. - \frac{3}{4} \frac{(1 + \lambda)^2}{(\alpha - 1)(\alpha + \lambda)} - \frac{1}{8} \frac{(1 + \lambda)^4}{(\alpha - 1)^2(\alpha + \lambda)^2} \right], & \text{for } \frac{1 - \lambda + \sqrt{2}(1 + \lambda)}{2} < \alpha; \end{aligned}$$

(b) for  $\lambda \leq (3 - 2\sqrt{2})$ :

$$\begin{aligned} \sigma_{\text{ion}} &= 0, & \text{for } \alpha < \left( \frac{\sqrt{2} - 1}{2} + \lambda \frac{\sqrt{2} + 1}{2} \right) \\ &= \frac{\pi q_0}{3 u^2} \frac{1}{\alpha^2} \left[ \frac{3}{8} \frac{(1 + \lambda)^2}{\alpha + 1} - \frac{1 + 2\sqrt{2}}{2(3 + 2\sqrt{2})} - \frac{\lambda^2}{2} \frac{\alpha - 2(\alpha^2 - \lambda)^{1/2}}{[\alpha - (\alpha^2 - \lambda)^{1/2}]^2} \right], & \text{for } \left( \frac{\sqrt{2} - 1}{2} + \lambda \frac{\sqrt{2} + 1}{2} \right) < \alpha < \left( \frac{\sqrt{2} + 1}{2} + \lambda \frac{\sqrt{2} - 1}{2} \right) \\ &= \frac{\pi q_0}{3 u^2} \frac{1}{\alpha^2} \left\{ 5 + \frac{3}{8} \frac{(1 + \lambda)^2}{\alpha + 1} - \frac{3}{4} \frac{(1 + \lambda)^2}{(\alpha - 1)(\alpha + \lambda)} + \frac{1 + \lambda}{2} \left[ \frac{\alpha - \lambda(3\alpha - 4)}{4(\alpha - 1)^2} - \frac{4\alpha - 1 + 3\lambda}{4(\alpha + \lambda)^2} \right] - \frac{(1 + \lambda)^4}{8(\alpha - 1)^2(\alpha + \lambda)^2} \right\}, \\ &\quad \text{for } \alpha > \frac{\sqrt{2} + 1}{2} + \lambda \frac{\sqrt{2} - 1}{2}. \end{aligned}$$

These expressions can be seen to be functions only of the velocity and mass ratios, aside from the factor  $1/u^2$ . This observation yields the scaling law quoted in the text. The fact that the same scaling law applies when the cross section is averaged over a hydrogenic distribution can be ascertained in a similar fashion by writing the expression for the case  $\frac{1}{2}mv_2^2 \neq u$ , and noting that the result after integration over the velocity distribution will be a function of  $E_1/u$  and  $\lambda$  only, aside from the  $1/u^2$  factor.

For  $\lambda \ll 1$ , these expressions simplify considerably:

$$\begin{aligned} \sigma_{\text{ion}} &= 0, & \text{for } \alpha < \frac{1}{2}(\sqrt{2} - 1) \\ &\simeq \frac{\pi q_0}{3 u^2} \frac{1}{\alpha^2} \left\{ 2\alpha^3 - \frac{1 + 2\sqrt{2}}{2(3 + 2\sqrt{2})} + \frac{3}{8(\alpha + 1)} \right\}, & \text{for } \frac{\sqrt{2} - 1}{2} < \alpha < \frac{\sqrt{2} + 1}{2} \\ &\simeq \frac{\pi q_0}{3 u^2} \frac{1}{\alpha^2} \left[ 5 + \frac{3}{8(\alpha + 1)} + \frac{\alpha}{8(\alpha - 1)^2} - \frac{4\alpha - 1}{8\alpha^2} - \frac{1}{8\alpha^2(\alpha - 1)^2} - \frac{3}{4\alpha(\alpha - 1)} \right], & \text{for } \alpha > \frac{1}{2}(1 + \sqrt{2}). \end{aligned}$$

For  $(m_e/m_1)E_1 \gg u$ , the cross section behaves as

$$\sigma_{\text{ion}} \rightarrow \frac{5\pi}{3} \frac{(z_1 z_2 e^2)^2}{\lambda u E_1},$$